MOEM

Modern Electronic Materials 2019; 5(4): 181–185
DOI 10.3897/j.moem.5.4.52932

Research Article

Structure formation by hot extrusion of thermoelectric bismuth chalcogenide solid solution rods

Vladimir T. Bublik[1], Mikhail G. Lavrentev[1,2], Vladimir B. Osvenskii[3], Yuri N. Parkhomenko[1,3], Nataliya Yu. Tabachkova[1,4]

1 National University of Science and Technology MISiS, 4 Leninsky Prospekt, Moscow 119049, Russia
2 RMT Ltd, 46 Warshavskoe Shosse, Moscow, 115230, Russia
3 JSC «Giredmet», 5-1 B. Tolmachevsky Per., Moscow 119017, Russia
4 A.M. Prokhorov General Physics Institute, Russian Academy of Sciences,38 Vavilova Str., Moscow 117942, Russia

Corresponding author: Nataliya Yu. Tabachkova (ntabachkova@gmail.com)

Received 27 June 2019 ♦ **Accepted** 12 November 2019 ♦ **Published** 31 December 2019

Citation: Bublik VT, Lavrentev MG, Osvenskii VB, Parkhomenko YuN, Tabachkova NYu (2019) Structure formation by hot extrusion of thermoelectric bismuth chalcogenide solid solution rods. Modern Electronic Materials 5(4): 181–185. https://doi.org/10.3897/j.moem.5.4.52932

Abstract

Major advantage of extruded Bi_2Te_3 based thermoelectric materials is high mechanical strength compared with that of melt-crystallized materials. Mechanical properties are of special importance for thermogenerator module applications where thermogenerator branches may undergo elevated thermal stresses due to large temperature differences at the modules. Since extrusion is typically a high-temperature process the structure of extruded materials is controlled by the plastic deformation in multiple slip systems resulting in the formation of a final deformed structure. The grain orientations are predominantly such that the most probable cleavage plane orientation is parallel to the extrusion axis. Recovery processes occur simultaneously and different recrystallization stages may take place. In the latter case the deformed texture may be destroyed.

Structure evolution along the extruded rod of $Bi_2Se_{0.3}Te_{2.7}$ ternary solid solution was studied with metallography and X-ray diffraction. Extrusion was interrupted for the study and so the specimen was a whole rod the initial part of which was the extrusion billet and the final part was the as-extruded material. The structure of the material is formed by competitive processes of dislocation generation and annealing. The plastic deformation energy is the highest in the extruder zone of the rod. Both the hardening processes and the texture are controlled by the plastic deformation mechanism. Plastic deformation is accompanied by generation of defects that are most likely vacancy type ones.

Keywords

hot extrusion, thermoelectric material, bismuth chalcogenides, plastic deformation

1. Introduction

The current status of research on thermoelectric materials and its main worldwide trends have been described quite thoroughly in reviews [1–6]. Low-temperature thermoelectric materials based on bismuth and antimony chalcogenide solid solutions have been the focus of researchers' attention over decades [7]. These materials are indispensable for the fabrication of devices and heat removal and near-room temperature control systems, although they can also be used in power generator units operated at below 300 °C. Bismuth telluride based solid solutions are the most produ-

ced and demanded materials in the world's thermoelectric materials markets. Low-temperature thermoelectric materials are grown by zone melting, Czochralski or Bridgman methods. However hot extrusion is in fact the most widely used growth process allowing the fabrication of desired shape rods with sufficiently high thermoelectric figure of merit *Z*. Major advantage of extruded Bi_2Te_3 based thermoelectric materials is high mechanical strength compared with that of melt-crystallized materials. Mechanical properties are of special importance for thermogenerator module applications where thermogenerator branches may undergo elevated thermal stresses due to large temperature differences at the modules [8–10]. Since extrusion is typically a high-temperature process the structure of extruded materials is controlled by the plastic deformation in multiple slip systems resulting in the formation of a final deformed structure. [11–14]. The grain orientations are predominantly such that the most probable cleavage plane orientation is parallel to the extrusion axis. Recovery processes occur simultaneously and different recrystallization stages may take place. In the latter case the deformed texture may be destroyed. Below we discuss structure evolution, dislocation density and texture pattern along the extruded rod of low-temperature *n* conductivity thermoelectric material.

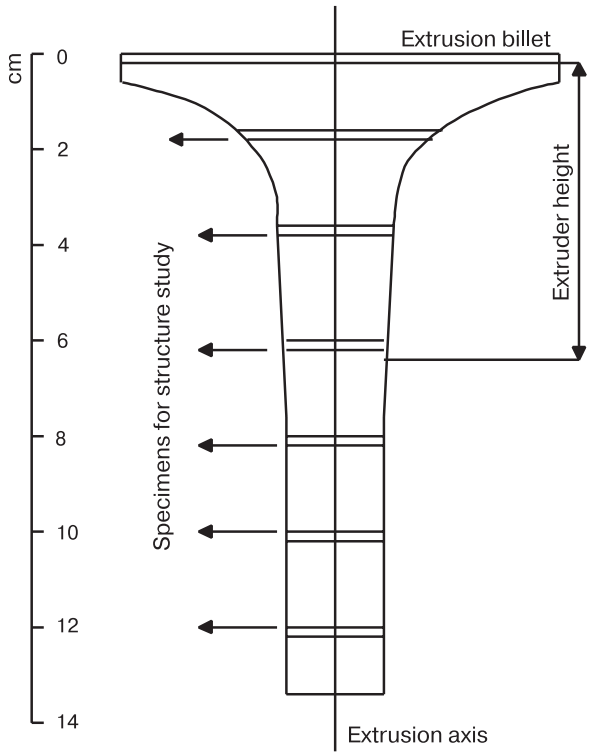

Figure 1. General appearance of extruded rod and specimen cutting scheme for X-ray diffraction study.

2. Experimental

Structure evolution along the extruded rod of $Bi_2Se_{0.3}Te_{2.7}$ ternary solid solution was studied with metallography and X-ray diffraction.

Extrusion was interrupted for the structure evolution study and so the specimen was a whole rod the initial part of which was the extrusion billet and the final part was the as-extruded material (Fig. 1). The extrusion billet diameter was 85 mm and the initial powder size was up to 500 μm. The material was extruded at 450 °C. The inner die diameter changed gradually, the die diameter and height being 20 and 60 mm, respectively.

The rod was cut along the extrusion axis for metallographic microstructure study.

For studying the texture and grain deformation by X-ray diffraction the specimens were cut from the extruded rod perpendicular to the extrusion axis. The texture was analyzed with the method of inverse pole figures **(IPF)**. The IPFs were plotted based on the diffraction patterns for the cross-sections perpendicular to the extrusion axis for evaluating the probability of coincidence between poles for different planes with the extrusion axis. The statistical weights of the poles were calculated with normalization by theoretical reflection intensities. Grain deformation was evaluated from Bragg peak broadening.

3. Results and discussion

Figure 1 shows schematic of specimen cutting from the extruded rod. The thermal field was such that the temperature was the highest in the extrusion billet zone. The process was interrupted when the as-extruded material at the die output was more than 65 mm in length counting from the rod beginning, i.e., the heat and mechanical impact patterns for these zones were the same as in a conventional process.

Figure 2 shows texture (left) and microstructure (right) evolution along the extrusion axis. The extrusion billet (Fig. 2*a*, *c*) has the as-cast texture for which the cleavage planes are parallel to the specimen surface, i.e., perpendicular to the extrusion direction. In the transient zone (in the extruder) the as-cast texture is destroyed and contains no predominant grain orientation (Fig. 2*b*, *g*). Deformation of the hot extruded material occurs by plastic flow leading to grain refinement. Plastic flow initiates in the central part of the rod, closer to the extrusion axis. Predominant $(11\bar{2}0)$ and $(10\bar{1}0)$ deformation texture forms at the extruder output (Fig. 2*c*, *h*) in which the cleavage planes are oriented along the extrusion axis. The texture does not undergo any major changes in the rest of the extruded rod (Fig. 2*d–j*). The porosity inherent to the extrusion billet is eliminated gradually simultaneously with texture formation. The specimen first output from the extruder had the lowest porosity (Fig. 2*e*, *j*).

Extrusion deformation in pressed $Bi_2Te_{2.7}Se_{0.3}$ alloy billets occurs mainly by grain boundary and dislocation slip in the basal (0001) and pyramidal $(10\bar{1}5)$ planes. Basal plane slip is preferential at any temperatures up to near the melting point due to bond anisotropy [15]. Basal plane slip occurs most likely by an inter-pack mechanism and

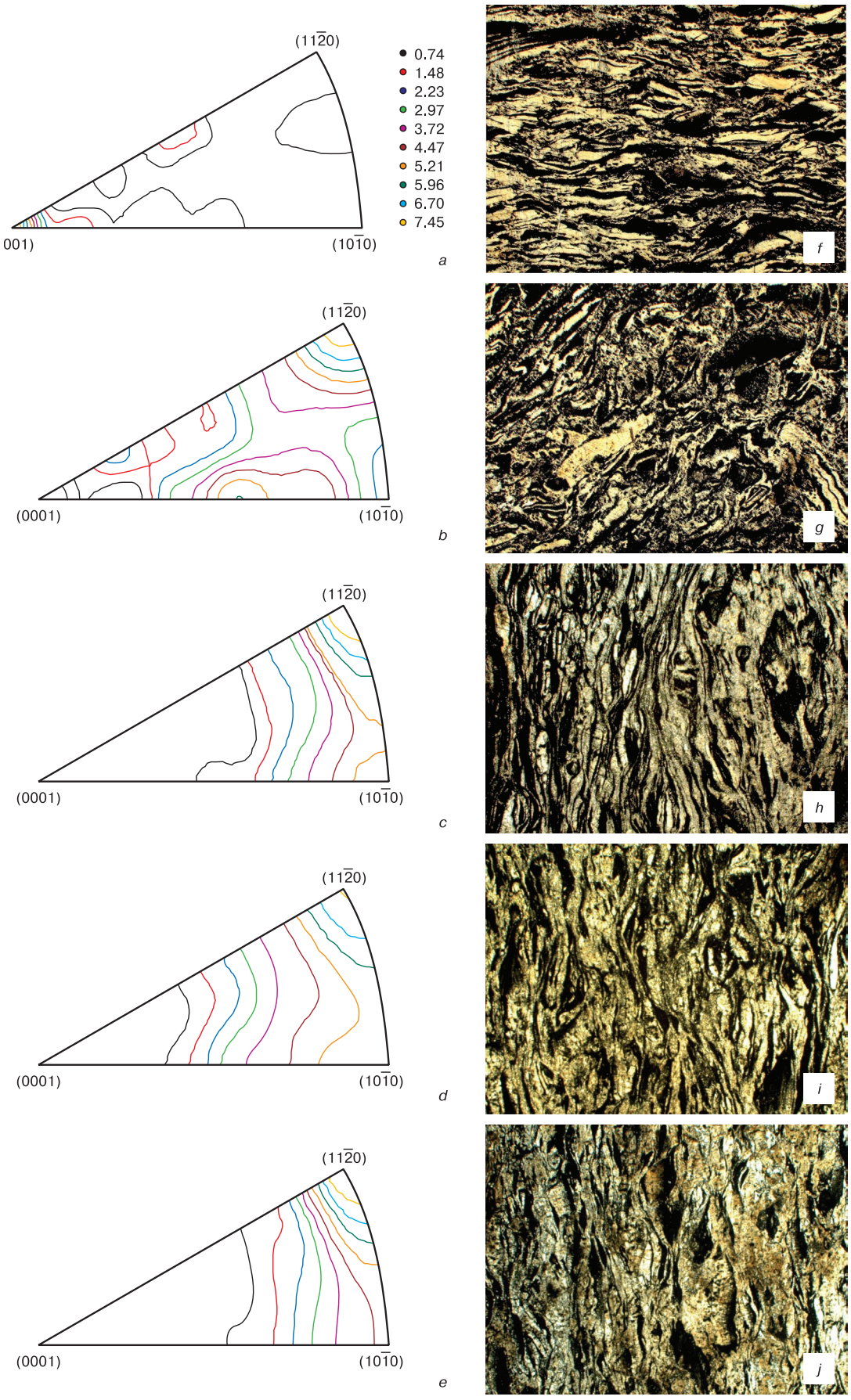

Figure 2. (*a–e*) Texture and (*f–j*) microstructure evolution along extrusion axis: (*a* and *f*) extrusion billet, (*b* and *g*) 2 cm, (*c* and *h*) 6 cm, (*d* and *i*) 10 cm and (*e* and *j*) 12 cm from extruded rod beginning.

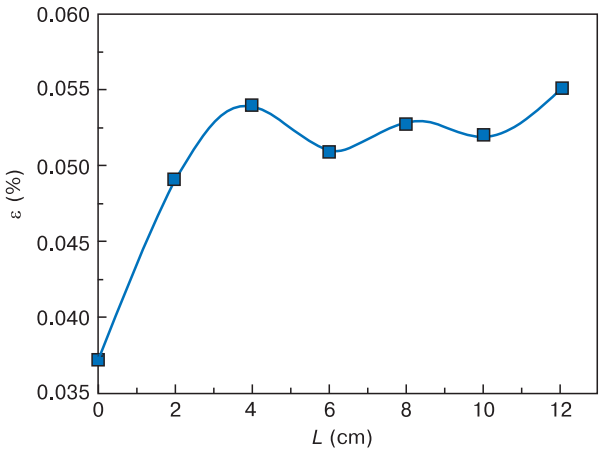

Figure 3. Evolution of microdeformation ε for different cut planes along extruded rod length *L*.

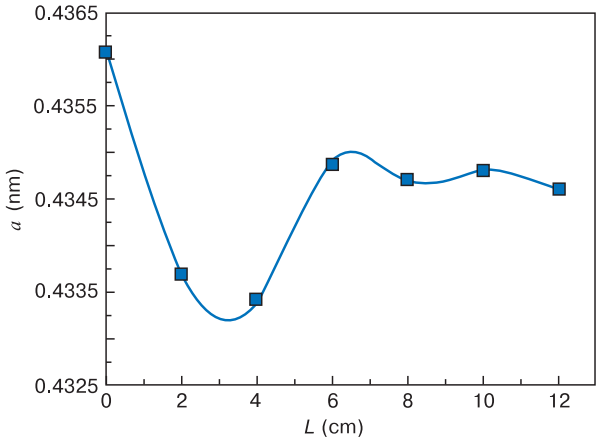

Figure 4. Lattice parameter evolution along extruded rod length *L*.

produces a $(11\bar{2}0)$ axial texture in which the basal planes are predominantly arranged parallel to the extrusion axis.

The concentration of defects in the grains was evaluated based on X-ray diffraction peak broadening. The X-ray diffraction peaks of the specimens cut out perpendicular to the extrusion axis were broadened due to the dislocation-induced microdeformations. Microdeformation evolution in specimens cut from different extruded rod zones is shown in Fig. 3.

Plastic deformation in the specimens is manifested by a permanent increase in the dislocation density until the transient zone in the extruder. After a certain deformation degree the flow stress no longer depends on the deformation degree, i.e., the specimen enters the steady state flow stage. The flow stress then reaches the highest value and decreases due to the intense development of dynamic recrystallization, producing a peak in the curve. The difference between dynamic and static recrystallization is that dynamically recrystallizing grains with low dislocation densities undergo hardening during further growth because of the persistent deformation. Grain growth at the extruder output is well illustrated by the microstructure images shown in Fig. 2. Since for sufficiently high degrees of hot deformation the deformation resistance depends not on the deformation degree but on the deformation rate [16], the strongest deformation occurs in the zones first output from the extruder at a specific extrusion rate because the deformation of the growing grains in these zones is predominant over annealing. Defects are intensely annealed simultaneously with deformation.

Figure 4 shows lattice parameter evolution in the ternary solid solution along the extruded rod.

The lattice parameter corresponding to the ternary solid solution composition $Bi_2Se_{0.3}Te_{2.7}$ is only the case for the rod zone corresponding to the initial extrusion stage at which the material is still inside the die. Selected area X-ray spectral analysis shows that the composition (within the measurement error) is the same along the rod and hence the decrease in the lattice parameter is caused by defect formation during extrusion.

The minimum lattice parameter corresponds to the maximum microdeformation zone (Fig. 3). Most likely point defects of predominantly vacancy type are generated in that zone as a result of multiple dislocation slip and grain boundary migration during recrystallization [17].

4. Conclusion

The structure formation pattern during hot pressing suggests that both grain deformation and texture are controlled by the type of plastic deformation. Plastic deformation is accompanied by generation of point defects that are most likely vacancy type ones. The structure develops under the conditions of competition between dislocation generation and annealing. The plastic deformation energy is the highest in the extruder zone of the rod. A structure containing a large number of dislocations and point defects forms as a result.

Acknowledgments

The work was financially supported by Russian Basic Research Fund, Grant No. 18-02-00036.

References

1. Snyder G.J., Toberer E.S. Complex thermoelectric matherials. *Nature materials*, 2008; 7: 105–114. https://doi.org/10.1038/nmat2090

2. Lan Y., Minnich A.J., Chen G., Ren Z. Enhancement of thermoelectric figure-of-merit by a bulk nanostructuring approach. Advanced

Functional Materials, 2010; 20(3): 357–376. https://doi.org/10.1002/adfm.200901512

3. Zebarjadi M., Esfarjani K., Dresselhaus M.S., Ren Z.F., Chen G. Perspectives on thermoelectrics: from fundamentals to device applications. *Energy Environ. Sci.*, 2012; 5: 5147–5162. https://doi.org/10.1039/C1EE02497C
4. Martín-González M., Caballero-Calero O., Díaz-Chao P. Nanoengineering thermoelectrics for 21st century: Energy harvesting and other trends in the field. *Renewable and Sustainable Energy Reviews*, 2013; 24: 288–305. https://doi.org/10.1016/j.rser.2013.03.008
5. Gonçalves1a A.P., Godart C. New promising bulk thermoelectrics: intermetallics, pnictides and chalcogenides. *The European Physical Journal B*, 2014; 87: 42. https://doi.org/10.1140/epjb/e2014-40989-3
6. Zhi-Gang Chena, Guang Hana, Lei Yanga, Lina Chenga, Jin Zou. Nanostructured thermoelectric materials: Current research and future challenge. *Progress in Natural Science: Materials International*, 2012; 22(6): 535–549. https://doi.org/10.1016/j.pnsc.2012.11.011
7. Scherrer H., Scherrer S. Thermoelectric properties of bismuth antimony telluride solid solutions. Thermoelectrics Handbook: Macro to Nano; Rowe, D.M. (Ed.). CRC Taylor and Francis: Boca Raton (FL, USA), 2012.
8. Zheng Y., Zhang Q., Su X., Xie H., Shu S., Chen T., Tan G., Yan Y., X. Tang, Uher C., Snyder G.J. Mechanically Robust BiSbTe Alloys with Superior Thermoelectric Performance: A Case Study of Stable Hierarchical Nanostructured Thermoelectric Materials. *Adv. Energy Mater.*, 2015; 5: 1401391. https://doi.org/10.1002/aenm.201401391
9. Ravi V., Firdosy S., Caillat T., Brandon E., Van Der Walde K., Maricic L., Sayir A. Thermal expansion studies of selected high-temperature thermoelectric materials. *J. Electron. Mater.*, 2009; 38: 1433–1442. https://doi.org/10.1007/s11664-009-0734-2
10. Sootsman J.R., Pcionek R.J., Kong H., Uher C., Kanatzidis M.G. Strong reduction of thermal conductivity in nanostructured PbTe prepared by matrix encapsulation. *Chem. Mater.*, 2006; 18(21): 4993–4995. https://doi.org/10.1021/cm0612090
11. Junyou Yang, Rougang Chen, Xi'an Fan, Wen Zhu, Siqian Bao, Xingkai Duan. Microstructure control and thermoelectric properties improvement to n-type bismuth telluride based materials by hot extrusion. *J. Alloys Compd.*, 2007; 429(1–2): 156–162. https://doi.org/10.1016/j.jallcom.2006.04.030
12. Keshavarz M.K., Vasilevskiy D., Masut R.A., Turenne S. *p*-type bismuth telluride-based composite thermoelectric materials produced by mechanical alloying and hot extrusion. *J. Electron. Mater.*, 2013; 42: 1429–1435. https://doi.org/10.1007/s11664-012-2284-2
13. Lognoné Q., Gascoin F., Lebedev O.I., Lutterotti L., Gascoin S., Chateigner D. Qualitative texture analysis of spark plasma textured *n*-Bi_2Te_3. *J. Am. Ceram. Soc.*, 2014; 97: 2038. https://doi.org/10.1111/jace.12970
14. Xu Z.J., Hu L.P., Ying P.J., Zhao X.B., Zhu T.J. Enhanced thermoelectric and mechanical properties of zone melted *p*-type $(Bi,Sb)_2Te_3$ thermoelectric materials by hot deformation. *Acta Mater.*, 2015; 84: 385–392. https://doi.org/10.1016/j.actamat.2014.10.062
15. Dubrovina A.N., Teut A.O. Studying the dependence of the structure and properties of the extruded material on the particle size of the initial powder. *Izv. AN SSSR. Neorgan. materialy*. 1990; 26(6): 1199–1202. (In Russ.)
16. Novikov I.I., Stroganov G.B., Novikov A.I. *Metallovedenie, termoobrabotka i rentgenografiya* [Metallurgy, heat treatment and radiography]. Moscow: MISiS, 1994, 480 p. (In Russ.)
17. Gorelik S.S., Dobatkin S.V., Kaputkina L.M. *Rekristallizatsiya metallov i splavov* [Recrystallization of metals and alloys]. Moscow: MISiS, 2005, 432 p. (In Russ.)